Microporous Materials

DOI: 10.1002/anie.200704790

A Route to Microporous Materials through Oxidative Pillaring of Micas**

Alexander Baumgartner, Katrin Sattler, Jürgen Thun, and Josef Breu*

Dedicated to Professor Armin Weiß on the occasion of his 80th birthday

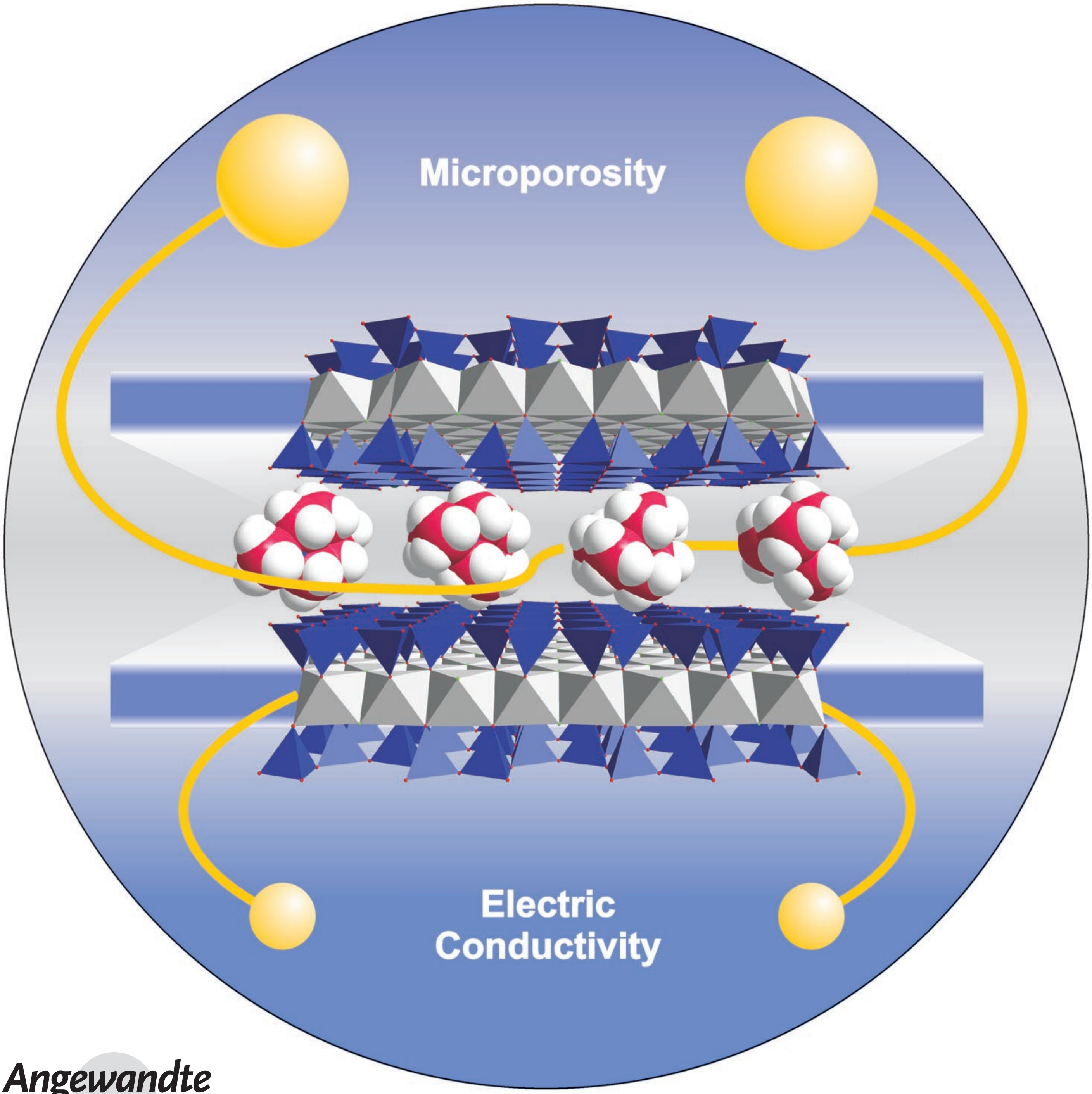

Owing to their eminent economical importance as molecular sieves, as storage materials, or as (shape-)selective heterogeneous catalysts, porous materials continue to draw attention in the fields of chemistry, physics, and material sciences. The field of porous materials has long been dominated by microporous inorganic solids like zeolites, aluminum phosphates, and gallium phosphates,[1] but more recently it was supplemented by mesoporous systems, mainly based on silica,[2] and by MOFs (metal–organic frameworks).[3] Besides these well-established classes, the intercalation of large complexes (pillars) in the interlayer of ionic lamellar materials provides an appealing and flexible route to microporous materials (pillared interlayered solids).[4,5] Especially intercalated layered silicates are promising compounds,[6,7] for example, for applications as (photo-)catalysts[8,9] or as sensor materials.[10] While these pillared layered clays (PILCs) are not as stable as zeolites in high-temperature applications, they provide unique features that ascribe a large potential to this class of materials. Since the pillars contribute to the pore surface of the whole PILC system (Figure 1), the major advantage of PILCs is the vast variability of possible (molecular) pillars with respect to size, shape, or additional functionality like chirality, catalytic activity, or hydrophobicity. Moreover, the pore diameter may in principle be adjusted over a wide range by controlling the cation-exchange capacity and thus the intermolecular distance of the pillars.

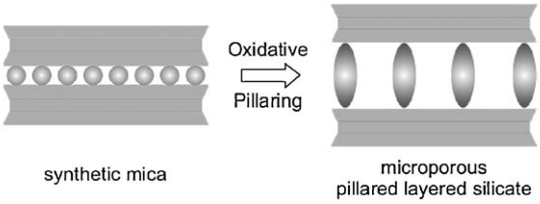

Figure 1. Pillaring concept of layered silicates.

In the past, the appealing concept of pillaring of layered silicates was severely hampered by deficiencies of the natural hosts used as starting materials. Natural clays are nanocrystalline, display fringed edges, and suffer from structural disorder and inhomogeneity in the charge density of the layers. All these aspects are detrimental for a well-defined porosity as they are responsible for the broad pore size distribution observed with pores ranging from micro- to mesopores.[11]

We present herein a structurally well-ordered, coarse-grained PILC $[(Me_2DABCO^{2+})_{0.22}Fe^{2+/3+}{}_{1.85}Li_{0.90}Si_4O_{10}F_2$ ($Me_2DABCO^{2+} = N,N$-dimethyl-1,4-diazabicyclo[2.2.2]octane dication)] which displays well-defined micropores. It is based on the synthetic layered silicate Cs-tainiolite ($Cs_{0.98}Fe^{2+}{}_{1.93}Li_{1.01}Si_4O_{10}F_2$), which shows charge homogeneity and no structural disorder in contrast to naturally occurring, swellable layered silicates. Additionally, this three-dimensional periodic structure can be maintained during the topotactical intercalation reaction, resulting in a well-defined microporous interlayer space. Unlike natural micas, which show no intracrystalline reactivity owing to the high layer charge, this synthetic mica readily undergoes cation exchange by an oxidative intercalation mechanism. Concomitantly with cation exchange, the layer charge is reduced all the way to the range of smectites by oxidation of structural Fe^{2+} ions (see reference [12] for details).

Owing to the high selectivity of the organic pillar for the interlamellar space, Me_2DABCO^{2+} quantitatively replaces Cs^+ as the interlayer cation. According to X-ray powder diffraction measurements, the interlayer distance is enlarged from 10.69 to 14.41 Å by this topotactic reaction. The unit cell volume is increased considerably from 512.4 to 689.1 Å^3 upon pillaring (Table 1). Surprisingly, this 34% increase in volume during intercalation of the pillar is accomplished while preserving the three-dimensional phase relation of the silicate layers (Figure 2). The powder X-ray diffraction pattern of the Me_2DABCO-tainiolite can be indexed and refined in *C*2*m* (No. 12; Table 1). The composition of the PILC was determined by LA-ICP-MS (LA = laser ablation, ICP = inductively coupled plasma) and CHN elemental analysis to be $(Me_2DABCO^{2+})_{0.22}Fe^{2+/3+}{}_{1.85}Li_{0.90}Si_4O_{10}F_2$.

Table 1: Refined unit cells from powder X-ray diffraction.

Compound	*a* [Å]	*b* [Å]	*c* [Å]	β [°]	*V* [Å^3]
Cs-tainiolite	5.273(3)	9.123(5)	10.800(5)	99.488(7)	512.4(14)
Me_2DABCO-tainiolite	5.261(3)	9.091(7)	14.520(6)	97.062(9)	689.2(21)

Physisorption measurements were performed with Ar/Ar(l). The adsorption/desorption isotherm (Figure 3) is almost horizontal in the p/p_0 region of the meso- and

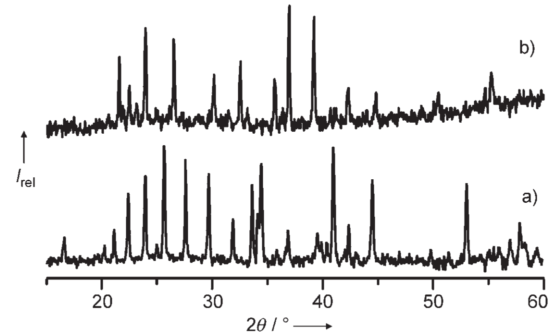

Figure 2. Powder X-ray diffraction pattern of a) Cs-tainiolite and b) Me_2DABCO-tainiolite.

---

[*] A. Baumgartner, K. Sattler, J. Thun, Prof. Dr. J. Breu
Lehrstuhl für Anorganische Chemie I
Universität Bayreuth
Universitätsstr. 30, 95447 Bayreuth (Germany)
Fax: (+49) 921-552-788
E-mail: Josef.Breu@uni-bayreuth.de

[**] This work was financially supported by the graduate school "Structure, Reactivity and Properties of Oxide Materials" within the Elitenetzwerk Bayern and the Deutsche Forschungsgemeinschaft (DFG, BR1408/5). We thank the Bayerisches Geoinstitut, Bayreuth for LA-ICP-MS measurements.

Supporting information for this article is available on the WWW under http://www.angewandte.org or from the author.

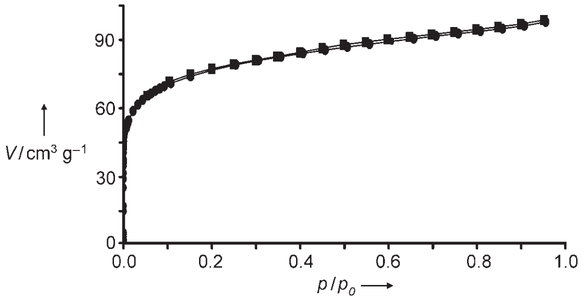

Figure 3. Physisorption isotherm (Ar/Ar(l)) of Me_2DABCO-tainiolite (● adsorption, ■ desorption, *V* under standard conditions).

macropores with no hysteresis observed. Therefore, it can be concluded that Me_2DABCO-tainiolite is a purely microporous system. Applying the BET equation, the surface area of the intercalated compound is determined to be 247 $m^2 g^{-1}$, which is as high as BET surfaces typically recorded for nanocrystalline zeolites (208 $m^2 g^{-1}$ for ZSM-5, crystal size 15 nm[13]).

To deduce the pore diameter of the microporous Me_2DABCO-tainiolite by physisorption, a nonlocal DFT model was applied (software Quantachrome Autosorb 1 version 1.52, Ar on zeolite/silica, cylindrical pores, equilibrium model[14]). The calculated pore diameter is in the range of 5 to 7 Å (Figure 4). The narrow pore diameter distribution is consistent with the high degree of ordering observable in the powder XRD pattern of Me_2DABCO-tainiolite (Figure 1 b). The organic pillar intrudes into the corrugated surface of the silicate layers on both sides of the interlamellar space and thus cross links consecutive layers (Figure 5). Thus, a regularly structured system of micropores is generated, resulting in the observed narrow pore diameter distribution.

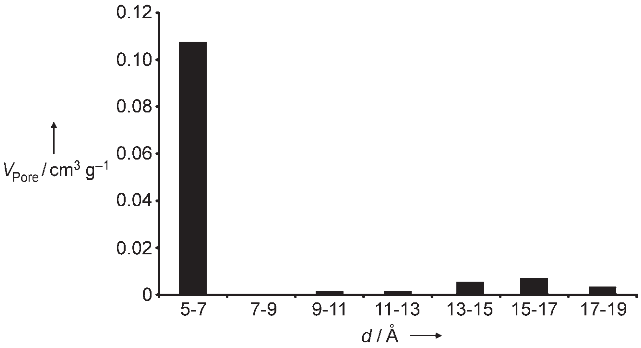

Figure 4. Histogram of pore diameter *d* of Me_2DABCO-tainiolite; V_{Pore}: pore volume under standard conditions.

The lack of stacking faults allows in-depth characterization of this PILC by a single-crystal structure refinement, which reveals structural details that are not accessible for intercalation compounds of naturally occurring and hydrothermally synthesized layered silicates, which all suffer from turbostratic disorder (consecutive layers are stacked randomly shifted and rotated with respect to each other). The structure refinement delivers valuable information about not only the structure of the silicate layer itself, but also the nature of the stacking of consecutive layers and, most importantly, the host–pillar interaction.

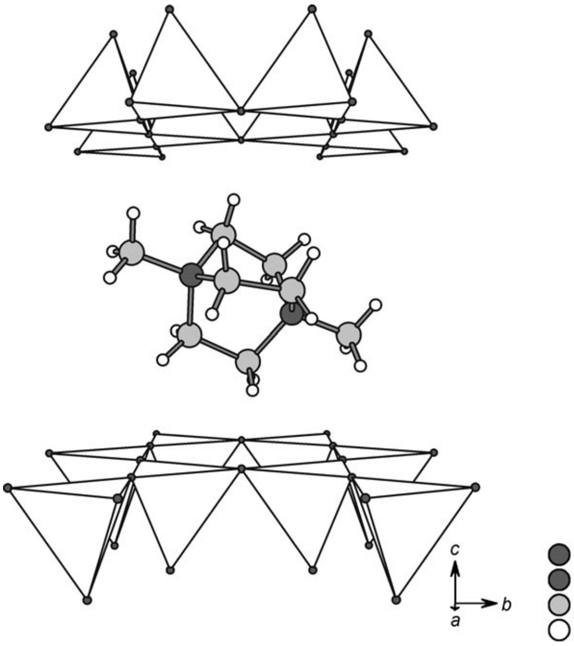

Figure 5. Results of the X-ray single-crystal refinement (tetrahedral layer of the layered silicate and Me_2DABCO^{2+} in the interlayer space).

As expected, the 2:1 silicate layers indeed prove to be rigid building blocks. All bond lengths and angles within the layers agree well with the values observed for the starting mica structure.[12] While many other silicates are known with more flexible layers[15] or which can easily be delaminated,[16] it is this pronounced rigidity of the sandwichlike 2:1 structure that allows the successful pillaring with preservation of crystallinity; as mentioned above, the stacking of the layers preserves the monoclinic symmetry. The hexagonal cavities of the two layers enclosing the interlamellar space are arranged exactly opposite of each other by the cross-linking pillar.

Unscrambling the orientation of the pillars is a bit more difficult. In the microporous material only about a quarter of the hexagonal cavities are actually occupied. Moreover, the surface of the trioctahedral host lattice displays a high hexagonal pseudosymmetry. Consequently, the X-ray beam averages over all possible positions, and the electron density in the interlamellar space appears rather blurred. Therefore, it was necessary to carry out a rigid-body refinement on the pillar. To verify the refinement, the orientation of the pillar was additionally investigated by molecular dynamics (MD) simulations. The pillar orientations obtained after geometry optimization of all saved frames of the simulations compared very well with the minima found by X-ray structure refinement. Figure 5 illustrates the orientation of the pillar molecule Me_2DABCO^{2+} in the interlayer space. The pillar is oriented with its C_3 axis tilted by approximately 24° against the *ab* plane. While two of the C_2H_4 handles protrude into the silicate layers, the third one is in the plane of the interlamellar space.

On the basis of these results, an estimation of the pore diameter of the microporous interlayer space is possible. Considering the site occupation factor of 0.22 for the pillars, the average intermolecular distance between the pillars is expected to be 11.7 Å. The pillar molecules are cylindrical with a van der Waals (vdW) diameter of 5.6 Å and a length of 8.8 Å. Taking the tilting angle into account, the projection of the latter onto the *ab* plane is approximately 8 Å. Thus, it may be deduced that the vdW gap between the pillars is in the range of 3.7 to 6.1 Å. The vdW thickness of the silicate layers is 9.7 Å,[17] which leads to a vdW gap between the silicate layers of 4.7 Å. Combining all assumptions, the pore diameter is estimated to be in the range of 4–6 Å, which is in good agreement with the physisorption measurements.

In summary, it can be stated that with microcrystalline synthetic micas that still provide sufficient intracrystalline reactivity by oxidative cation exchange, the appealing concept of pillaring may be revitalized. The intercalation of Me_2DABCO^{2+} into synthetic Cs-tainiolite yields a material with microporosity comparable to zeolites with respect to both narrow pore size distribution and total pore volume. In contrast to PILCs made of naturally occurring and hydrothermally synthesized layered silicates, this compound is three-dimensionally ordered and reveals in-depth structural details. Owing to the high structural Fe content, the PILC described here provides a size-selective, shape-selective, and at the same time electronically conducting[12] framework. Its applicability as a sensor for redox-active ambient gas species (e.g. CO) will be explored in future work. Also, it will be investigated whether the pillar density and hence pore diameter may be tuned by an electrochemical adjustment of the Fe^{2+}/Fe^{3+} ratio.

Experimental Section

Cs-tainiolite was synthesized as described previously.[12] After synthesis, the compound was annealed for 20 days at 875 °C in a gas-tight molybdenum crucible to release structural strain and to increase crystal size.

For intercalation, the annealed Cs-tainiolite (500 mg) was treated hydrothermally for 24 h at 120 °C using a 0.125 M solution of $Me_2DABCOCl_2$ (4×10 mL) followed by four additional exchanges with a 0.250 M solution of $Me_2DABCOCl_2$ (10 mL each).

The XRD patterns were recorded with a STOE Stadi P powder diffractometer (transmission, $Cu_{K\alpha}$ radiation, Ge monochromator, linear PSD). The relatively high background is due to X-ray iron fluorescence. To control the amount of pore water, the samples were equilibrated for 14 days over a saturated LiCl solution (15 % relative humidity).

Single-crystal X-ray diffraction data were collected at 298 K on a STOE IPDS diffractometer with graphite-monochromated $Mo_{K\alpha}$ radiation (0.71073 Å). Intensity data were collected in 90 frames (1° step per frame, 30 min per frame) for a rather small ($0.156 \times 0.117 \times 0.03$ mm^3) but carefully examined crystal which was free from diffuse streaks from stacking disorder. A numerical absorption correction was applied by using the program X-RED32 based on a crystal description optimized using equivalent reflections with X-SHAPE[18] ($\mu(Mo_{K\alpha}) = 2.35$ mm^{-1}). Refined unit cell: monoclinic, space group $C2m$ (No. 12), $a = 5.2727(11)$, $b = 9.1290(18)$, $c = 14.542(3)$ Å, $\beta = 96.95(3)°$, $V = 694.9(2)$ Å^3, $Z = 2$, $\rho_{calcd} = 2.157$ g cm^{-3}. The refinement on F^2 was carried out using SHELXL97[19]: $F(000) = 445$, $2\theta_{max} = 59.6°$, 1166 reflections collected of which 704 were unique ($R_{int} = 0.0729$). Final R indices for 387 reflections with $I > 2\sigma I$: $R1 = 0.0932$, $wR2 = 0.2408$. Atoms of the silicate layer were refined anisotropically, Me_2DABCO^{2+} was treated as a rigid body with a common isotropic displacement parameter for all atoms.[20]

The utilized LA-ICP-MS system consisted of an Elan DRC-e quadrupole mass spectrometer (Perkin Elmer Instruments) attached to a Geolas M 193-nm ArF excimer laser system (Coherent/Lambda Physik). Technical details about this system can be found in the literature.[21] Samples were pressed to pellets without any additives and ablated with a laser beam (5–20 mm diameter, 10 Hz, 25 kV). The sample chamber was flushed with helium gas (1 L min^{-1}), to which Ar was added on the way to the ICP-MS. Signals were recorded with five sweeps per second, and instrument background was measured for 30 s before each analysis. Integrated signal intensities were referenced to NIST SRM 610 glass according to routines described elsewhere.[22] Element ratios were turned into stoichiometric coefficients by normalization to $Si_{4.00}$.

Quantification of the pillars was done by elemental analysis (Elementar vario el III). To reach higher combustion temperatures (1150 °C) that are necessary for complete oxidation of the pillars, the combustion tube was filled with tungsten(VI) oxide granules. Additionally, the combustion time in pure oxygen was increased up to 3 min (O_2 index 5).

The physisorption measurements were performed by using a Quantachrome Autosorb 1 at Ar(l) temperature (87.45 K) with Ar. The substance was previously dried three days at 150 °C in high vacuum over P_2O_3.

A 100-ps MD run (NVT ensemble, Berendsen thermostat, 0.1-fs time step, frame output every 1000 steps) was performed at 600 K with fixed clay geometry. The Discover module and the augmented CVFF force field (CVFF-aug) in the MS Modeling 4.0 suite of programs were used.[23] Finally, clustered frames were locally optimized. The point charges for the Me_2DABCO^{2+} molecule were fitted to the electrostatic potential using the DMol^3 module[24] (GGA-PW91 functional and the DNP basis set) while the charges of the clay atoms were assigned from the force field.

Received: October 16, 2007

Keywords: intercalations · layered compounds · microporous materials · silicates

[1] A. K. Cheetham, G. Ferey, T. Loiseau, *Angew. Chem.* **1999**, *111*, 3466–3492; *Angew. Chem. Int. Ed.* **1999**, *38*, 3268–3292.

[2] F. Hoffmann, M. Cornelius, J. Morell, M. Fröba, *Angew. Chem.* **2006**, *118*, 3290–3328; *Angew. Chem. Int. Ed.* **2006**, *45*, 3216–3251.

[3] S. Kaskel, F. Schüth, M. Stocker, *Microporous Mesoporous Mater.* **2004**, *73*, 1.

[4] M. Behrens, O. Riemenschneider, W. Bensch, S. Indris, M. Wilkening, P. Heitjans, *Chem. Mater.* **2006**, *18*, 1569–1576.

[5] M. S. Whittingham, Y. N. Song, S. Lutta, P. Y. Zavalij, N. A. Chernova, *J. Mater. Chem.* **2005**, *15*, 3362–3379.

[6] J. D. Gale, A. K. Cheetham, R. A. Jackson, C. R. A. Catlow, J. M. Thomas, *Adv. Mater.* **1990**, *2*, 487–490.

[7] R. A. Schoonheydt, T. Pinnavaia, G. Lagaly, N. Gangas, *Pure Appl. Chem.* **1999**, *71*, 2367–2371.

[8] J. M. Thomas, *Philos. Trans. R. Soc. London Ser. A* **1990**, *333*, 173–207.

[9] M. Ogawa, K. Kuroda, *Chem. Rev.* **1995**, *95*, 399–438.

[10] U. Guth, S. Brosda, J. Schomburg, *Appl. Clay Sci.* **1996**, *11*, 229–236.

[11] H. Nijs, M. De Bock, N. Maes, E. F. Vansant, *J. Porous Mater.* **1999**, *6*, 307–321.

[12] R. Mariychuk, A. Baumgartner, F. E. Wagner, A. Lerf, A. Dubbe, R. Moos, J. Breu, *Chem. Mater.* **2007**, *19*, 5377 – 5387.

[13] W. Song, R. W. Justice, C. A. Jones, V. H. Grassian, S. C. Larsen, *Langmuir* **2004**, *20*, 8301 – 8306.

[14] M. Thommes in *Nanoporous Materials: Science and Engineering (*Eds.: G. Q. Lu, X. S. Zhao), Imperial College Press, London, **2004**.

[15] A. Corma, V. Fornes, S. B. Pergher, T. L.M Maesen, J. G. Buglass, *Nature* **1998**, *396*, 353 – 356.

[16] H. K. Jeong, S. Nair, T. Vogt, L. C. Dickinson, M. Tsapatsis, *Nat. Mater.* **2003**, *2*, 53 – 58.

[17] J. Breu, W. Seidl, A. J. Stoll, K. G. Lange, T. U. Probst, *Chem. Mater.* **2001**, *13*, 4213 – 4220.

[18] STOE & Cie GmbH. STOE X-Area V 1.35. **2006**, Darmstadt.

[19] G. M. Sheldrick, SHELXS-97, Program for the Solution of Crystal Structures, Universität Göttingen, **1997**; G. M. Sheldrick, SHELXL-97, Program for the Refinement of Crystal Structures, Universität Göttingen, **1997**.

[20] Further details on the crystal structure investigations may be obtained from the Fachinformationszentrum Karlsruhe, 76344 Eggenstein-Leopoldshafen, Germany (fax: (+49) 7247-808-666; e-mail: crysdata@fiz-karlsruhe.de), on quoting the depository number CSD-418801.

[21] D. Günther, R. Frischknecht, C. A. Heinrich, H. J. Kahlert, *J. Anal. At. Spectrom.* **1997**, *12*, 939 – 944.

[22] H. P. Longerich, S. E. Jackson, D. J. Gunther, *J. Anal. At. Spectrom.* **1996**, *11*, 899 – 904.

[23] Accerlys. Material Studio, Release 4.0. **2006**, Accelrys Software Inc., San Diego.

[24] B. Delley in *Modern Density Functional Theory* (Ed.: J. M. Seminario), Elsevier, Amsterdam **1995**, pp. 221 – 254.